MIT-CTP 4422

Instanton in a thermal bath and melting of a pion string

Johanna Karouby*
Center for Theoretical Physics and Department of Physics,
Massachusetts Institute of Technology, Cambridge, Massachussetts 02139, USA

The instanton production for out-of-equilibrium scalar fields in a thermal bath of photons is computed in the thin-wall limit. Such a process accurately describes the melting and the breaking of a pion string via bubble nucleation. In a plasma, the topologically unstable pion string becomes metastable so that it can decay through quantum tunneling. In the following, the decay of the false vacuum into the true vacuum in the core of the string is used to quantify the quantum decay rate of the string into two strings. The cylindrically and spherically symmetric instantons are found. As a result of the tunneling, the string core melts, vacuum bubbles propagate along the string at almost the speed of light and baryon production could occur via skyrmion production.

arXiv:1212.1723v1 [hep-th] 7 Dec 2012

I. INTRODUCTION

Topological defects are widely observed in condensed matter: for instance, string-like defects form when the vacuum manifold is such that the first homotopy group is non-trivial. In the case of the pion string, the circle of minima formed by the charged fields, $|\pi_c| = \eta$, encloses the defect line if finite temperature effects are considered [1] [2]. In the same way, non-singular point-like topological objects, such as skyrmions, are observed in liquid crystals and form when the third homotopy group of the vacuum manifold $\mathcal{M}$, is non trivial: $\pi_3(\mathcal{M}) \neq 1$[3] [4]. Following these examples, the early Universe should contain such topological defects due to the rapid phase transition it undergoes while cooling down. As a consequence, topological defects can play an important role in early universe cosmology (see e.g. [5–7] for overviews). On one hand, particle physics models which yield defects such as domain walls which have problematic and unobserved effects can be ruled out. On the other hand, string-like topological defects may help explain certain cosmological observations. They could contribute to structure formation or generate primordial magnetic fields which are coherent on cosmological scales [8].

In the following we focus on a specific period of the early Universe, namely the QCD phase transition. A big challenge in cosmology is to relate the models we have to the physics of the standard model of particles. Here, the linear sigma model Lagrangian, which describes pions at low energy, provides a starting point for our analysis. In this set-up, the pion string is topologically unstable due to the fact that the vacuum manifold symmetry group, O(4), is too large. In a previous attempt to make the pion string stable, we found that the presence of a photon bath enhances the stability of the string for a certain range of temperatures by effectively reducing the vacuum manifold to a circle [1] [2]. However, [1] indicates this string is not stable but rather metastable. As a result, the system can move to the lowest energy state, the true vacuum, through a process known as bubble nucleation. The quantum tunneling from the false to the true vacuum is studied by finding the instanton solution. For the pion string, this mechanism also generates new field configurations, skyrmions, via pair production which can be interpreted as baryon-anti-baryon pair production in the context of the Skyrme model [9][10][11].

Instanton production and string breaking have been widely studied in literature, mainly from a "world-sheet" point of view [12–17]. Here our approach is different and more closely resembles more the study of 1st order phase transitions in the early universe [18–22]. We are interested in the pion string below the chiral phase transition temperature of QCD, and thus we only deal with out-of-equilibrium scalar fields. Considering a thermal bath of photons coupled to the system yields a metastable effective potential and allows the presence of embedded topological defects (see [23],[24] for a review of embedded topological defects). Our goal is to compute the tunneling probability from the false vacuum to the true vacuum of the theory in order to quantify the decay rate of the string through bubble nucleations. The string will be truly stable and thus have an impact on cosmology, only if the decay rate is bigger than the Hubble parameter H: $H < \Gamma$ where Γ is the decay rate of the string. In general, different bubble shapes are possible and the total decay rate should be the sum of the decay rate into all possible configurations. In order to estimate the decay rate of the string into two strings, we mainly focus on the semi-classical "bounce" computation by Coleman in the thin-wall approximation [25]. Making these approximations allows us to estimate the euclidean action of the instanton for different symmetry configurations.

In the first subsection, we review the pion string and introduce its finite temperature effective potential. Due to the shape of the potential, the string is stable above a certain temperature, metastable at smaller temperatures and classically unstable below T_0. In the following subsection, we set one ansatz for each pair of fields describing the string: (16) and (17) in order to represent the string instanton before ($t = -\infty$) and after tunneling ($t = 0$). We then show the resulting euclidean action.
Keeping cylindrical symmetry of the equations of mo-

---

*karoubyj@mit.edu

tion necessary to get straight strings, implies that we are left with three possible configurations: two are cylindrical and one is spherical. In section IV, we study each of them in turn: first, the O(2) symmetric instanton, then the O(3) one, and finally the spherical one. In general, the more symmetry an instanton has, the smaller Euclidean action it has, so that it contributes more to the decay rate. Finally, we compare the value of the different instanton contributions, estimate the decay rate for precise values of the linear sigma model parameters and conclude on how likely the melting process is.

II. EFFECTIVE POTENTIAL FOR THE PION STRING

A. The pion string

As a toy model for the analytical study of the stabilization of embedded defects by plasma effects we consider the chiral limit of the QCD linear sigma model, involving the sigma field σ and the pion triplet $\vec{\pi} = (\pi^0, \pi^1, \pi^2)$, given by the Lagrangian

$$\mathcal{L}_0 = \frac{1}{2}\partial_\mu\sigma\partial^\mu\sigma + \frac{1}{2}\partial_\mu\vec{\pi}\partial^\mu\vec{\pi} - \frac{\lambda}{4}(\sigma^2 + \vec{\pi}^2 - \eta^2)^2\,, \quad (1)$$

where η^2 is the ground state expectation value of $\sigma^2 + \vec{\pi}^2$. In the following, the potential in (1) is denoted by V_0.

Two of the scalar fields, the σ and π_0, are electrically neutral, the other two are charged. Introducing the coupling to electromagnetism, it is convenient to write the scalar field sector $\mathcal{L}$ of the resulting Lagrangian in terms of the complex scalar fields

$$\pi^+ = \frac{1}{\sqrt{2}}(\pi^1 + i\pi^2)\,, \;\; \pi^- = \frac{1}{\sqrt{2}}(\pi^1 - i\pi^2)\,. \quad (2)$$

According to the minimal coupling prescription we obtain

$$\mathcal{L} = \frac{1}{2}\partial_\mu\sigma\partial^\mu\sigma + \frac{1}{2}\partial_\mu\pi^0\partial^\mu\pi^0 + D_\mu^+\pi^+ D^{\mu -}\pi^- - V_0\,, \quad (3)$$

where $D_\mu^+ = \partial_\mu + ieA_\mu$, $D_\mu^- = \partial_\mu - ieA_\mu$ and V_0 is a Mexican-hat potential: $V_0 = \frac{\lambda}{4}(\sigma^2 + \vec{\pi}^2 - \eta^2)^2$. Note that the effective pion-photon interactions appear through the covariant derivative in (3).

When one considers a specific configuration where $\sigma^2 + {\pi_0}^2 = \eta^2$ and $\pi^+ = \pi^- = 0$, the vacuum manifold S^3 reduces to S^1 and string configurations exist but are not topologically stable since $\pi_1(S^3) = 1$. From now on we will work with 2 complex scalar fields, one combining the charged pions, $\pi_c = \pi^1 + i\pi^2$ and the other representing the uncharged fields, $\phi = \sigma + i\pi_0$.

In order to make the pion string stable let us consider a thermal bath of photons in contact with the fields. At temperatures below the chiral symmetry breaking temperature for the linear sigma model, $T_{ch} = \sqrt{2}\eta$, we assume that there is only one field in equilibrium, the gauge field A_μ, and four scalar fields out-of-equilibrium: two combined into one complex charged field, π_c and two neutral fields forming the pion string combined into the complex field, ϕ. Above T_{ch}, thermal fluctuations are so big that the σ field condensate goes to zero and there is no string solution. In the case at hand, below the confinement temperature, non-thermal pions dominate so that a zero temperature computation for the effective potential (4) suffices. The number density of pions being very small compared to the one of photons, we can consider that photons are indeed in thermal equilibrium while the pions are not. In addition, from a cosmological perspective, the temperature must also be below the freeze-out temperature, T_f, in order for the fields to leave thermal equilibrium.

Considering temperatures below T_{ch} and T_f give rise to a new effective potential at finite temperatures [1]:

$$\begin{aligned} V_{eff}(\phi, \pi_c, T) \;=\; & \frac{\lambda}{4}(|\phi|^2 + |\pi_c|^2 - \eta^2)^2 - \frac{\pi^2 T^4}{45} + \frac{e^2|\pi_c|^2T^2}{12} \\ & - \frac{e^3|\pi_c|^3 T}{6\pi} - \frac{e^4|\pi_c|^4}{16\pi^2}\left[\ln\left(\frac{e|\pi_c|e^{\gamma_E}}{4\pi T}\right) - \frac{3}{4}\right] \quad (4) \end{aligned}$$

where γ_E is the Euler-Mascheroni constant. For this potential, the vacuum manifold forms a circle in phase space: $|\phi|^2 = \eta^2$ and $|\pi_c| = 0$. As mentioned earlier, such a system admits string solutions: in our case, at temperature below the confinement scale, an embedded neutral string exists. As shown in Fig.1, above the critical temperature, T_1, the potential barrier is infinite in the charged pions direction and no tunneling occurs. For temperatures between T_c and T_1, $|\pi_c| = 0$, is the true VEV so that the pion string is stable. For both these cases, the neutral string is quantum mechanically stabilized.

However, for temperatures between T_0 and the critical temperature $T_c = \frac{\sqrt{6\lambda}\eta}{e}\frac{1}{\sqrt{1-\frac{e^4}{3\lambda\pi^2}}}$, the system exhibits a 1st order phase transition due to the negative cubic term in the potential. As a result, the zero charged pion condensate becomes metastable: $|\pi_c|$ is in a false vacuum so that we expect quantum tunneling. In other words, this quantum tunneling occurs when the charged fields tunnel to a non-vanishing expectation value in the true ground state, $|\pi_c| = v'$ where $v'$is the true VEV (remember that there are two charged fields so this is actually a "true vacuum manifold", a circle of radius v'). As a consequence, the core of the neutral string melts and the string breaks at various locations. Indeed, these quantum tunneling effects can happen anywhere on the string, resulting in the nucleation of bubbles at the breaking points. Let us now take a closer look at the potential giving rise to this quantum tunneling.

B. Potential in the decoupling limit at high-temperatures

In the high-temperature expansion, $\frac{|\pi_c|}{T} \ll 1$ so that we can neglect higher-order terms of the full effective potential (4) and drop the logarithmic part:

$$V_{eff}(\phi, \pi_c, T) \simeq \frac{\lambda}{4}(|\phi|^2+|\pi_c|^2-\eta^2)^2+\frac{e^2|\pi_c|^2}{12}T^2-\frac{e^3|\pi_c|^3}{6\pi}T \tag{5}$$

Note that for simplicity, we also drop the purely temperature dependent part of the potential, $\frac{-\pi^2 T^4}{45}$.

The crucial point is that there are four fields so that the tunneling process is, in general, extremely difficult to study. Restricting ourselves to the core of the string, we can consider $|\phi| = 0$ during the tunneling process since by continuity, the neutral fields at the center of the string vanishes. In its core, the string does not have any potential barrier in the ϕ direction since ϕ vanishes identically. It is thus well justified to consider quantum tunneling only along the π_c direction. In other words, it is enough to consider the tunneling of only the charged fields, keeping the neutral ones equal to zero. This greatly simplifies our task from a computational point of view since, as show in Fig.1, the potential becomes a function of π_c only.

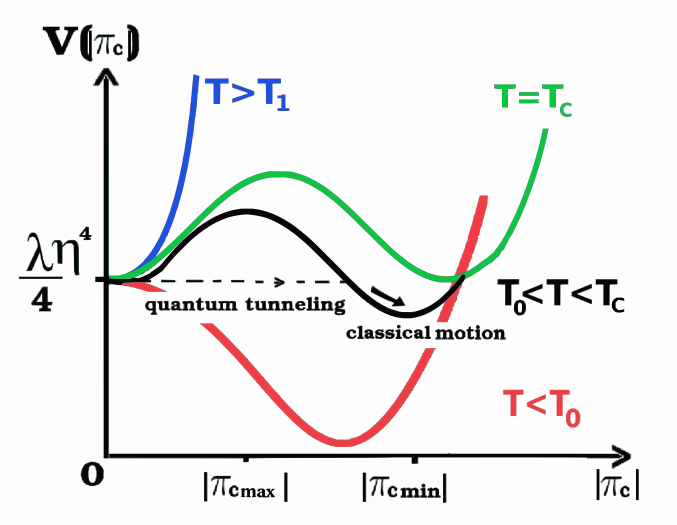

FIG. 1: Finite temperature effective potential in the core of the string. The horizontal dashed line indicates the tunneling of the string from its initial configuration (where the charged fields vanish everywhere) to the exit point after quantum tunneling. The arrow toward the minimum indicates the classical decays towards the true vacuum which occurs after quantum tunneling.

In order to study the potential (5) it is useful to rewrite it in terms of powers of the charged field

$$V(\pi_c, T) = D(T^2 - T_o^2)\pi_c^2 - ET\pi_c^3 + \frac{\lambda}{4}\pi_c^4 \tag{6}$$

where the coefficients are given by

$$D = \frac{e^2}{12} \quad E = \frac{e^3}{6\pi} \quad T_o^2 = \frac{6\lambda\eta^2}{e^2} \tag{7}$$

and where, for simplicity we set the initial potential energy to 0 instead of $\frac{\lambda\eta^4}{4}$. In order to know when tunneling can occur, we will find at which temperature a true vev exists, and above which temperature the barrier is infinite. Neglecting Hubble expansion for now, quantum tunneling occurs at constant energy so that the field emerges at an exit point, π_c^* after which it classically rolls down the potential as show in Fig.1.

In order to find the extrema of the potential we impose $\frac{\partial V}{\partial \pi_c} = 0$ and find, in addition to the false vacuum $\pi_c = 0$, two other solutions

$$\pi_c \mp = \frac{1}{2}[\frac{3ET}{\lambda} \pm \sqrt{9\frac{E^2T^2}{\lambda^2} - \frac{8D}{\lambda}(T^2 - T_0^2)}] \tag{8}$$

The first point, π_c+, is a maximum and the second one, π_c- is a minimum which corresponds to the true vacuum. Note that these solutions exist only for $\frac{9E^2T_1^2}{\lambda} < 8D\left(T_1^2 - T_0^2\right)$, meaning $T < T_1$ with $T_1^2 = \frac{8D\lambda T_0^2}{8D\lambda - 9E^2} = \frac{6\lambda^2\eta^2}{e^2\lambda - \frac{6}{\pi^2}e^6}$. Requiring T_1^2 to be positive imposes the following condition:

$$\lambda \geq \frac{3e^4}{8\pi^2}$$

In order to get the exit point after tunneling, π_c^*, we search for the zeros of the potential:

$$\pi_c^* = \frac{2ET}{\lambda}\left(1 - \sqrt{1 - \frac{\lambda D}{E^2}\left(1 - \frac{T_0^2}{T^2}\right)}\right) \tag{9}$$

Whenever the potential vanishes at 3 points, there will be a decay to the lower energy vacuum. This is the case whenever

$$T^2 \geq \frac{\lambda D}{E^2}\left(T^2 - T_0^2\right) \Rightarrow T^2 \leq \frac{\lambda D T_0^2}{-E^2 + \lambda D} = T_c^2 \tag{10}$$

where

$$T_c^2 = \frac{T_0^2}{1 - \frac{e^4}{3\lambda\pi^2}} \tag{11}$$

is the critical temperature. As expected this critical temperature is smaller than T_1. As a consequence, the decay into two strings for $T > T_c$ won't occur and the initial single string configuration remains stable.
At $T = T_c$, the potential has two degenerate solutions $\pi_c = 0$ and $\pi_c = \pi_c^D$. Moreover, since the two vacua have the same energy, $V(\pi_c) = 0$, the exit point, π_c^*, becomes the degenerate vacuum:

$$\pi_c = 0 \quad \text{and} \quad \pi_c^*(T_c) = \pi_c^D(T_c) = \frac{2ET_c}{\lambda} \tag{12}$$

This configuration is the starting point of our instanton computation which involves the thin wall approximation.

Up to this point we have not yet shown which string configuration corresponds to the instanton. In attempt to do so, we now introduce an ansatz for the pion string and show the resulting action.

III. STRING INSTANTON

Instantons are classical solutions to the euclidean equation of motion with non-zero action. In order to study the quantum stability of the string against breaking, one can find the instanton configuration which corresponds to the tunneling from the false vacuum to the true one. In order to do so we first introduce an ansatz for the string solution.

A. Ansatz for the string cylindrical instanton

As an example, we present an ansatzt for the cylindrical string instanton which, as indicated by the name, has cylindrical symmetry around the string axis. Note that the cylindrical symmetry is the minimal symmetry required from the string equations of motion.

Let us consider an initial U(1) neutral string configuration lying on the z-axis which decays to two neutral U(1) strings. In our set-tup the initial configuration corresponds to infinite time: $t = \pm\infty$ whereas the tunneling occurs at $t = 0$

$$
\begin{aligned}
t: \qquad & \pm\infty \to 0 \\
(\phi_i, \pi_{ci}) &\to (\phi_b, \pi_{cb})
\end{aligned}
\tag{13}
$$

As a result, the solution "bounces" at $t = 0$ [25].

Starting with the Nielsen and Olesen static string [26] at $t = \pm\infty$ yields

$$
(\phi_i, \pi_{ci}) = (\eta f(\rho) e^{in\theta}, 0) \tag{14}
$$

where ρ is the distance to the core of the string, n the winding number and θ is the angle in the plane orthogonal to the string.

After tunneling, the string breaks so that two half-strings extend on each side of the z=0-plane. This intermediate configuration also called, bouncing point, occurs at $t = 0$. As shown in Fig.3, after tunelling, the field ϕ vanishes on the $z = 0$-plane by continuity in the vicinity of the z-axis since it also vanishes in the core of the initial and final strings. In order to keep the cylindrical symmetry of the system, we choose the patch where $\phi = 0$ to be a disk of radius ρ_0 centered on the origin

$$
\phi_b = \begin{cases} \eta f(\rho) e^{in\theta} \quad for\ z \neq 0\ and\ z = 0, \rho \geq \rho_0 \\ 0 \quad for\ z = 0\ and\ \rho < \rho_0 \end{cases} \tag{15}
$$

Thus, for the whole configuration to lie on the vacuum manifold around the string, the charged fields have to be turned on on the patch defined above

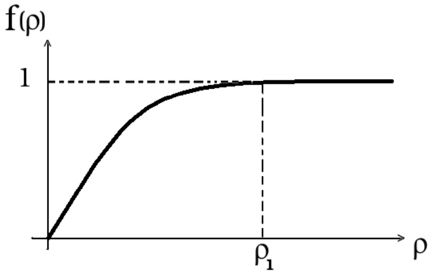

FIG. 2: Profile function for the Nielsen-Olesen string for winding number $n = 1$. Contrary to the case for $g_1(\rho)$ and $g_2(s)$, the derivative of $f(\rho)$ does not vanish at the origin $\rho = 0$ but would do so for $n > 1$.

$$
\begin{cases} \pi_{cb} = \eta\ for\ z = 0,\ \rho < \rho_0 \\ \pi_{cb} = 0\ for\ z \neq 0\ and\ z = 0,\ \rho > \rho_0 \end{cases} \tag{16}
$$

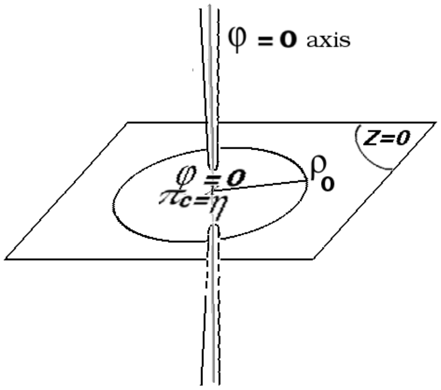

FIG. 3: Breaking of a string into two strings
The vertical axis represents the core of the string where the field ϕ vanishes. In the region of radius ρ_0 around the core of the string of the $z = 0$ plane, the charged pions turn on and take on their v.e.v, $\langle \pi_c \rangle = \eta$, while the field ϕ is still vanishing.

Let us now introduce a time dependance, assuming an extra O(2) symmetry in the (z, τ)-plane where, $\tau = it$, is the euclidean time. Our ansatz can now be written in terms of the new polar coordinate $s = \sqrt{\tau^2 + z^2}$

$$
\phi_{(}\tau, \rho, z, \theta) = \eta f(\rho) e^{in\theta} [g_1(\rho) + \sqrt{1 - g_1(\rho)^2} g_2(s)] \tag{17}
$$

$$
\pi_c(\tau, \rho, z, \theta) = \eta \sqrt{1 - g_1(\rho)^2} \sqrt{1 - g_2(s)^2} \tag{18}
$$

Note that two O(2) symmetries of the bounce solution coexist: one in (z, τ)-plane and one in the (ρ, θ)-plane so that $\phi_{(}\tau, \rho, z, \theta) = \phi_{(}\rho, s, \theta)$. Rotating back to Minkowski spacetime, yields one O(1,1) symmetry and one O(2) one.

The general boundary conditions to get a bounce are:

$$
\partial_\tau (\phi(\tau), \pi_c(\tau))_{\tau=0} = \partial_\tau (\phi_b, \pi_{cb}) = (0, 0) \tag{19}
$$

$$
\lim_{\tau \to \pm\infty} (\phi, \pi_c) = (\phi_i, \pi_{ci}) = (0, 0) \tag{20}
$$

The boundary conditions, (17)(18)(19)(20), yield the following conditions for $g_1(\rho)$ and $g_2(s)$:

$$g_1(0) = g_1(\rho \leq \rho_0) = 0 \ , g_1(\rho > \rho_0) = 1 \ , g_1'(0) = 0 \quad (21)$$

$$g_2(0) = 0 \ , g_2(\pm\infty) = 1 \ , g_2'(0) = 0 \quad (22)$$

where ’ denotes the derivative with respect to s (respectively ρ) since (19) holds at any point of space and we can thus substitute τ with s (respectively ρ).

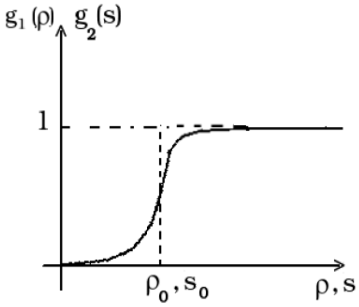

FIG. 4: Profile function for $g_1(\rho)$ and for $g_2(s)$
The profile function for $g_1(\rho)$ and $g_2(s)$ look the same. The initially value of g_1 cancels out and then jumps For the threshold value $\rho \geq \rho_0$, the function goes to 1 in order to have the charged pions turned on only inside the disk of radius ρ_0 at the bouncing point (t=0). The initial value of g_2 vanishes since $\phi(0) = 0$ and has a vanishing gradient corresponding to the bouncing point as seen in(22). It then jumps to 1 to come back to the single neutral string configuration at $t = +\infty$. In a similar way, we asymptotically reach the value 1 for the profile of each of the three functions $f,\ g_1\ and\ g_2$.

Let us evaluate the typical length scale of the quantum tunneling. To go from the initial configuration to the bounce one, the fields jump quantum mechanically during a very short transition time that one can estimate using Heisenberg uncertainty principle : $Et \sim \hbar$. The typical energy we consider is the energy of the core of the string: $E \sim \frac{\lambda}{4}\eta^4 V$ where V is the volume. Considering the width of the string, $w \sim (\sqrt{\lambda}\eta)^{-1}$, the volume of the initial cylinder inside the string is, $V \sim \pi w^2 s_0$ where s_0 is the height of the cylinder. We therefore obtain the typical tunneling length, $l \sim t \sim \frac{4\sqrt{\lambda}}{\pi\eta^2 s_0}$ in units where $\hbar = c = 1$. For s_0 big enough, $l < w$ and the assumption that tunneling occurs within the core of the string is consistent. Here s_0 corresponds to the point where the quantum jump occurs, meaning that we can infer that the profile of $g_2(s)$ has a sharp change at $s = s_0$. In a similar manner, we suppose that the profile of $g_1(\rho)$ has a sharp change at $\rho = \rho_0$ as show in Fig.4. Later, in section IV.A, we find the exact relationship between ρ_0 and s_0 in the thin-wall approximation case.

The effects of this quantum tunneling is to split the string. Indeed, the boundary of the cylindrical region separating the two strings expand vertically in a way that $z^2 - t^2 = s_0^2$. As a result the velocity of the wall is $v = \frac{dz}{dt} = \frac{\sqrt{z^2 - s_0^2}}{z}$ which, after a very short time, becomes the speed of light. As a consequence, the two newly formed strings quickly move away from each other along the z-axis at the speed of light and the core of the string melts.

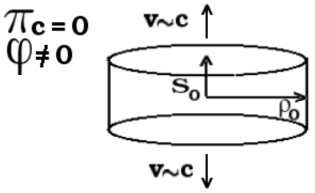

FIG. 5: Cylindrical shape for the instanton configuration
When one substracts the bounce action from the original string one, one is left with a cylinder of radius ρ_0 and height s_0 that is expanding vertically at the speed of light.

Let us now quantify the probability of the string breaking through quantum tunneling by computing the instanton euclidean action.

B. Euclidean action

Our initial problem includes four fields so that an infinite number of field space trajectories exist for the quantum tunneling problem. As a result, we need to choose a plausible trajectory. Here we introduce the decoupling limit in more precise terms. Let us define the new variable u: $u = \sqrt{\phi^2 + \pi_c^2}$ so that our initial fields are $\phi = usin(\theta)\ and\ \pi_c = ucos(\theta)$. In a schematic way, the quantum tunneling description is

$$\begin{aligned} t : 0 &\rightarrow \infty \\ configuration : bounce &\rightarrow stable\ string \\ \phi = usin(\theta) : 0 &\rightarrow \eta f(\rho) e^{in\omega} \\ \pi_c = ucos(\theta) : \pi_c^* &\rightarrow 0 \end{aligned} \quad (23)$$

so that $tan\theta = \frac{\phi}{\pi_c} : 0 \rightarrow \infty$.

The euclidean action for the string is now

$$S_E = 4\pi^2 \int \rho d\rho s ds \frac{1}{2}[(\frac{\partial_u}{\partial_s})^2 + (\frac{\partial_u}{\partial_\rho})^2 + u^2[(\frac{\partial_\theta}{\partial_s})^2 + (\frac{\partial_\theta}{\partial_\rho})^2] + 2V(u, \theta, T)]. \quad (24)$$

where we have neglected the winding gradient of the string. We can choose a specific trajectory for $\theta(\rho, s)$ that satisfies the boundary conditions (23). Restricting ourselves to the core of the string, $\phi = 0$ at any time. As a result, $tan\theta$ always vanishes in the decoupling limit.

We can now write the Euclidean action for the cylindrical string instanton described above:

$$S_E = 4\pi^2 \int \rho d\rho s ds \frac{1}{2}[(\frac{\partial_\phi}{\partial_s})^2 + (\frac{\partial_\phi}{\partial_\rho})^2 + \frac{1}{\rho^2} n^2 \phi^2] + 4\pi^2 \int \rho d\rho s ds [\frac{1}{2}[(\frac{\partial_{\pi_c}}{\partial_s})^2 + (\frac{\partial_{\pi_c}}{\partial_\rho})^2] + V(\phi, \pi_c, T)] \quad (25)$$

where the integral runs from 0 to ∞. According to Derrick's theorem, the energy configuration resulting from the gradient term due to the winding around the string, $\frac{1}{\rho^2}n^2\phi^2$ is infinite in more than one dimension. Fortunately, the introduction of gauge fields cure this problem and from this point of view, the action should be free of divergence.

Let us now estimate the analytical value of the instanton action and the corresponding string decay rate. In order to do so, we can use the thin-wall approximation close to the critical temperature, T_c.

IV. THIN-WALL APPROXIMATION

The thin-wall approximation allows to use a semi classical computation to estimate the production rate of thin-wall bubble and is valid when the potential is almost degenerate. For our potential (6), the approximation is valid for temperatures just below the critical temperature T_c. Therefore the first instantons formed correspond to thin-wall bubbles. At lower temperature, the thin wall approximation breaks and the wall becomes thick since the height of the barrier is small compared to the value of the potential at its minimum. Whether bubble nucleation occurs via thick or thin wall tunneling depends on how big the decay rate is in the thin wall case. If the decay rate is big enough, nucleation will proceed via thin-wall tunneling. If not, one can solve the thick-wall case which most likely requires numerics.

Let us consider our potential at temperatures where the difference in energy between the two minima is negligible. Since the 2 minima are almost degenerate, one can neglect the damping term in the equation of motion for the charged fields, π_c, so that

$$\frac{d^2\pi_c}{d\rho^2}+\frac{1}{r}\frac{d\pi_c}{d\rho}=V'(\pi_c) \tag{26}$$

becomes

$$\frac{d^2\pi_c}{d\rho^2}=V'(\pi_c)\simeq V'_D(\pi_c) \tag{27}$$

where $V_D(\pi_c)$ is the potential in the limit where the potential has an exact degeneracy ($\epsilon \sim 0$ or equivalently, $T \sim T_c$).

Let us now rewrite the potential (6) to make appear the thin-wall parameter ϵ, as in [27]

$$V(\pi_c)=\frac{\lambda}{4}\pi_c^2(\pi_c-\pi_c^D)^2-\frac{\lambda}{2}\epsilon\pi_c^D\pi_c^3 \tag{28}$$

$$where\ \epsilon=\frac{ET}{\sqrt{\lambda D}}\frac{1}{\sqrt{T^2-T_0^2}}-1=\sqrt{\frac{T_c^2-T_0^2}{T^2-T_0^2}}\frac{T}{T_c}-1 \tag{29}$$

$$and\ \pi_c^D(T)=2\sqrt{\frac{D}{\lambda}(T^2-T_0^2)} \tag{30}$$

Note as a consistency check that this potential vanishes at $\pi_c^D(T_c)$ since ϵ vanishes at the critical temperature and that the critical value $\pi_c^D(T_c)$ matches the one found in (12).

For this potential (28), the one-dimensional Euclidean action is

$$S_1=\int dx[\frac{1}{2}(\frac{\partial_\phi}{\partial_x})^2+V(\phi)]=\int_{\pi_c^D}^{0}d\phi[2V_D(\phi)]^{\frac{1}{2}}=\frac{(\pi_c^D)^3\sqrt{\lambda}}{6\sqrt{2}} \tag{31}$$

Making the temperature dependence explicit yields

$$S_1(T)=\frac{4}{3\sqrt{2}\lambda}[D(T^2-T_0^2)]^{3/2}=\frac{e^3}{18\sqrt{6}\lambda}[(T^2-T_0^2)]^{3/2} \tag{32}$$

Note that this action has mass dimension 3 since it is the one-dimensional action.

Another quantity, the potential energy density difference between the two minima, plays an important role in the computation of the action,

$$\Delta V=V(\pi_{cmin})=\frac{\lambda}{2}\epsilon(\pi_c^D)^4 \tag{33}$$

$$\Delta V=8(ET-\sqrt{\lambda D}\sqrt{T^2-T_0^2})[\frac{D}{\lambda}(T^2-T_0^2)]^{\frac{3}{2}}$$

Here, contrary to the Mexican hat potential case (with no cubic term) [25], ΔV, is not equal to the thin-wall parameter ϵ which is a dimensionless quantity that decreases with temperature (see Fig.6)

$$T=\frac{T_0}{\sqrt{1-\frac{e^4}{3\pi^2\lambda(\epsilon+1)^2}}}\ \text{and}\ \epsilon(T)=\sqrt{\frac{e^4}{3\pi^2\lambda}\frac{1}{1-\frac{T_0^2}{T^2}}}-1 \tag{34}$$

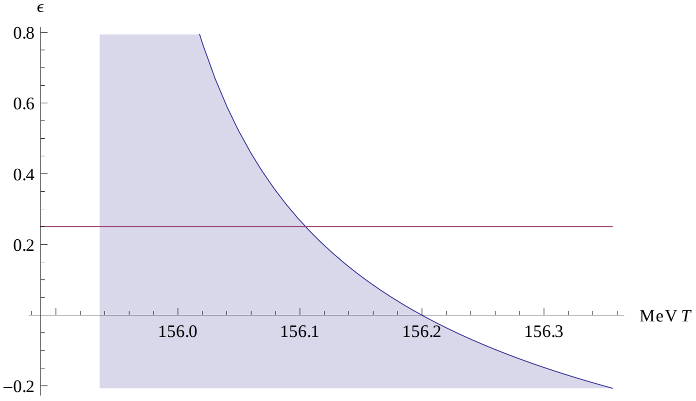

FIG. 6: Plot of the thin parameter, ϵ, as a function of temperature for $\lambda = 10e^4$, $e^2 = \frac{4\pi}{137}$, $\eta = 66.47MeV$. These parameters correspond to $T_0 = 155.936$ MeV, and the critical temperature equals to $T_c = 156.2$MeV. The thin-wall approximation is valid only in a narrow energy range (less than 1MeV) very close to T_c. The horizontal line represents a 25% threshold value (found in (48)) above which the thin wall approximation is not valid anymore. For the approximation, to be valid, ϵ must be much smaller than this threshold value. We see that the thin-wall parameter vanishes at the critical temperature.

From (29) and (34), we can see that the thin-wall parameter exactly vanishes at the critical temperature. Above, T_c, the second minimum of the potential is higher than the initial one so that the field is already in the true vacuum and no tunneling occurs: The thin-wall approximation does not make sense anymore and ϵ becomes negative. Far below T_c, the value of the thin wall parameter explodes and the approximation breaks down. As a consequence, the thin-wall approximation in only valid in the vicinity of T_c.

In order to evaluate the thickness of the bubble wall, one can solve the differential equation (27) where the damping term has been neglected. The solution close to $r \sim R$ (the radius of the bubble wall which we compute in the following) is [27]:

$$\pi_c(r) = \frac{1}{2}\pi_c^D[1 - tanh[\frac{r-R}{\delta}]] \tag{35}$$

where δ, the wall thickness, is equal to

$$\delta = \sqrt{\frac{8}{\lambda}}\frac{1}{\pi_c^D} = \frac{2\sqrt{6}}{e}\frac{1}{\sqrt{T^2 - T_0^2}} \tag{36}$$

and, as expected, the higher the temperature, the thiner the wall is.

Let us now use the thin-wall approximation and the physical quantities mentioned above to estimate the action for different instanton configurations.

A. Cylindrical Bounce: O(2)x O(2) symmetry

Let us come back to the string cylindrical instanton and compute the most probable configuration by using the thin-wall approximation described above and by extremizing the action. For this cylindrical case illustrated in Fig. 5, the action (25) simplifies to

$$\begin{aligned} S_{cyl} &= 4\pi^2 \int \rho d\rho s ds [\frac{1}{2}[(\frac{\partial_{\pi_c}}{\partial_s})^2 + (\frac{\partial_{\pi_c}}{\partial_\rho})^2] + V(\pi_c)] \\ &= 4\pi^2[\rho_0 s_0 S_2 - \frac{\rho_0^2}{2}\frac{s_0^2}{2}\Delta V] \end{aligned} \tag{37}$$

where S_2 is the 2-dimensional action that we approximated as: $S_2 \sim 4\delta S_1$, so that the action becomes

$$S_{cyl} = 4\pi^2 \rho_0 s_0 [4\delta S_1 - \frac{\rho_0 s_0}{4}\Delta V] \tag{38}$$

The first term is the gradient energy associated with the cylindrical wall and the second one corresponds to the vacuum energy in the interior of the cylinder.

In order to find the optimal dimension of the most likely nucleated cylinders, we look for the saddle points of the euclidean action

$$\frac{\partial_{S_E}}{\partial_\rho}|_{\rho_0} = 0 \; and \; \frac{\partial_{S_E}}{\partial_s}|_{s_0} = 0$$

The set of (ρ_0, s_0) that fulfills the above extremization constraint of the euclidean action form a curve in the $(\rho, s) - plane$: $\rho_0 s_0 = \frac{8\delta S_1}{\Delta V}$.
Plugging it back into (38) yields

$$S_{cyl} = 64\pi^2 \frac{\delta^2 S_1^2}{\Delta V} = \frac{64\pi^2}{2781}\frac{e^4}{\lambda^2}\frac{(T^2 - T_0^2)^2}{\Delta V} = \frac{128\pi^2}{9\epsilon\lambda} \tag{39}$$

The string will break at some point on the z=0 plane with a probability per unit volume

$$\frac{\Gamma_{sphere}}{V} \sim P_2 e^{-\frac{128\pi^2}{9\epsilon\lambda}} \tag{40}$$

where P_2 is a prefactor that we will estimate later. It is worth noting that in the thin-wall approximation $\epsilon \ll 1$, so that most of the contribution to the decay rate comes from the exponential part.
After, tunneling, the two strings immediately move away from each other along the z-direction at almost the speed of light. Moreover, the damping effect coming from the plasma pressure should not have a great effect since the string expand vertically and not radially.

There is another possibility for a cylindrical instanton: one that would expand radially rather than vertically (see Fig.7), the O(3) symmetric instanton.

B. Cylindrical Bounce: O(3) symmetry

Let us now introduce the O(3) cylindrical instanton which, when formed, would expanding radially in the plane orthogonal to the string. In this case, the gradient energy from the winding around the string and the pressure of the plasma should prevent this radial expansion to occur as shown in Fig.7. If no such physical effects would prevent radial expansion, the O(3) instanton should give a larger decay rate than the O(2) one because of its larger symmetry group.

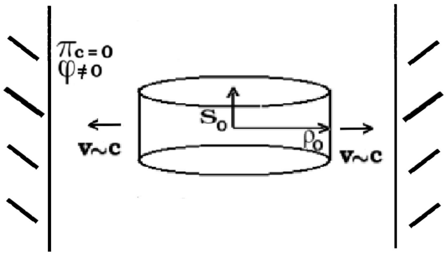

FIG. 7: Cylindrical shape of the $O(3)$ instanton configuration. When one removes the bounce action to the original string one, one is left with a cylinder of radius ρ_0 and height s_0 that should be expanding radially at the speed of light. The dashed walls on each side of the string represents the gradient energy from the string winding that prevents the radial expansion.

For the sake of generality, we now present some results that go beyond the thin-wall approximation [22].

The euclidean action for an O(3) bounce for purely thermal fields reads

$$\frac{S_3}{T} = 4.85\frac{M^3(T)}{E^2T^3}f(\alpha) \tag{41}$$

where $f(\alpha) = 1 + \frac{\alpha}{4}\left[1 + \frac{2.4}{1-\alpha} + \frac{0.26}{(1-\alpha)^2}\right]$,
$M^2(T) = 2D(T^2 - T_0^2)$ is the mass term and $\alpha = \frac{\lambda M^2(T)}{2E^2T^2}$. The approximation above is valid for any temperature between T_0 and T_c so that $f(\alpha)$ is correct with an accuracy about 2% when α goes from 0 to 1. Applying (41) to our case yields the dimensionless euclidean action

$$S_{cylrad} \sim 4.85\frac{z_0M^3(T)}{E^2T^2}f(\alpha) \tag{42}$$

where z_0 is the invariant height of the cylinder nucleated.

The physics in [22] differs from our pion string case where only the photons are in thermal equilibrium. However the result for the three dimensional Euclidean action still holds since the Lagrangians of both systems have the same form. The only difference is that, the O(3) symmetry applies to the three spatial directions (rotational invariance of the bubble nucleated), instead of two spatial plus one time component for the radially expanding cylinder (cylindrical configuration nucleated).

In general, the most probable configurations nucleated should be bubbles with an O(4) symmetry in the Euclidean plane. So, let us now have a closer look at the O(4) instanton.

C. Spherical Bounce: O(4) symmetry

In general, the most probable way for the charged fields to tunnel through the potential barrier is through the nucleation of bubbles (which have an O(4) symmetry in the Euclidean plane) due to the fact that O(4) is the largest possible symmetry group [25]. Here, the spherical bubble, which incorporates the cylindrical symmetry needed to get strings, should give the biggest decay rate. However, the two antagonist effects to bubble nucleation mentioned above, plasma pressure and string winding gradient, should prevent or restrict any radial expansion. Thus, we expect that once the bubbles form, they get deformed and propagate along the string.

Let us now take a closer look at the dynamics of the problem. The equation of motion for a spherical bounce in 4-dimension

$$\frac{d^2\pi_c}{dr^2} + \frac{3}{r}\frac{d\pi_c}{dr} = V'(\pi_c) \tag{43}$$

becomes the same as the cylindrical case since we do not consider the damping term in the thin wall approximation: $\frac{d^2\pi_c}{d\rho^2} = V_D'(\pi_c)$ where r and ρ are the radial distances in spherical and polar coordinates, respectively. Integrating over a 3-sphere of radius R yields

$$\begin{aligned} S_{sphere} &= \pi^2 \int r^3 dr[\tfrac{1}{2}(\tfrac{\partial_{\pi_c}}{\partial_r})^2 + V(\pi_c)] \\ &= -\tfrac{\pi^2}{2}R^4\Delta V + 2\pi^2R^3S_1 \end{aligned} \tag{44}$$

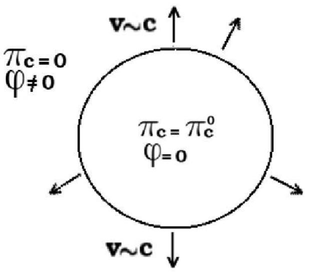

FIG. 8: Spherical shape for the instanton configuration
In the ideal case, a sphere of radius R is generated and expands radially at almost the speed of light

where R is the radius of the bubble in Euclidean space. As usual, we should extremize the action in order to determine the radius of the bubble nucleated: $\frac{\partial_{S_E}}{\partial_R} = 0$ and

$$R(T) = \frac{3S_1}{\Delta V} = \sqrt{\frac{3}{2e}}\frac{1}{\epsilon\sqrt{T^2 - T_0^2}} \tag{45}$$

Plugging back in the action yields

$$S_{sphere} = 27\pi^2\frac{S_1^4}{2\Delta V^3} = \frac{\pi^2}{48\lambda\epsilon^3} \tag{46}$$

Replacing ϵ by a function of temperature (28), one can see that $\frac{\partial_R}{\partial_T}$ is positive for any temperature below T_c so that the radius of the bubble increases with temperature. As a result, when the Universe expands and cools down, the pion string would generate bubbles of smaller size. Using the action we can finally write the decay rate per unit volume:

$$\frac{\Gamma_{sphere}}{V} \sim P_4 \exp[-\pi^2\frac{1}{48\ \lambda(\sqrt{\frac{e^4}{3\pi^2\lambda}\frac{T^2}{T^2-T_0^2}} - 1)^3}] \tag{47}$$

where P_4, the prefactor can be estimated on dimensional grounds. Therefore the decay rate decreases with temperature.

After tunneling in vacuum, the bubble radially expands at the velocity $v = \frac{d|\vec{x}|}{dt} = \frac{\sqrt{|\vec{x}|^2 - R^2}}{|\vec{x}|}$ which rapidly becomes the speed of light. However, in our case, the pressure the plasma exerts on the wall slows down this expansion.

Let us write now use the velocity we just found and write the energy of the bubble wall in the core of the string (otherwise we have to consider the neutral pion as well)

$$E_{wall} = 4\pi|\vec{x}|^2(S_1^{\pi_c})(1 - v^2)^{-\frac{1}{2}}$$

which finally reduces to

$$E_{wall} = 4\pi|\vec{x}|^3\frac{S_1^{\pi_c}}{R} = \frac{2\pi\epsilon}{27\lambda}|\vec{x}|^3e^4(T^2 - T_0^2)^2$$

As expected, when the temperature decreases, the energy of the wall decreases while the initial velocity of the bubble wall increases due to a smaller initial radius. In addition, the pressure exerted by the thermal bath is lower at smaller temperature and thus has a milder effects on slowing down radial expansion.

Let us now discuss our results and compare the O(4) instanton we just described with the O(2) instanton.

V. DISCUSSION AND NUMERICAL RESULTS

A. Prefactor estimate

In order to estimate the decay rate of the string, we made use of the semiclassical approximation which only applies when the instanton action is very small, $S_E \gg 1$. In addition, this approximation holds only if the radius of the bubble wall is much bigger than its thickness

$$\frac{3S_1}{\Delta V} \gg \sqrt{\frac{8}{\lambda}}\frac{1}{\pi_c^D} \tag{48}$$

or equivalently, $\epsilon \ll \frac{1}{4}$ *or* $T \gg \frac{1}{1-\frac{4e^4}{15\lambda\pi^2}}$.
In this regime, the tunneling rate is determined mainly by the action, and the value of the prefactor, P, can simply be estimated using dimensional analysis. According to [18], the prefactor, P in front of the exponential factor for the decay rate is of order

$$P_n{=}\sqrt{(\frac{S_E^n}{2\pi\hbar})}^n\sqrt{\frac{det[-\partial^2+V''(\pi_c^*)]}{det'[-\partial^2+V''(0)]}}{\sim}\sqrt{\frac{S_E^n}{2\pi\hbar}}^n V''(\pi_c^*)^2 \tag{49}$$

where det' denote the determinant computed with the zero eigenvalue omitted and n corresponds to the number of zero modes associated with translational invariance in euclidean space [28]. For the spherical case, $n = 4$, the cylindrical $O(3)$ case, $n = 3$ and the cylindrical $O(2) \times O(2)$ case, $n = 2$. S_E^n is the corresponding euclidean action for the $O(n)$ symmetric configuration. The prefactor computation for different symmetries of the instanton is more precisely discussed in [29][30].

In order to evaluate the potential, we compute the value of the potential close to the critical temperature $V''_{eff}(\pi_c^*) \sim V''_{eff}(\pi_c^D) \sim \frac{e\sqrt{T^2-T_0^2}}{\sqrt{6}}$ which, is of order T so that the total decay rate per unit volume has unit of T^4. Then, a quick estimate for the cylindrical and spherical instanton prefactor (49) yields

$$P_2{\sim}\frac{3.7e^2}{\lambda\epsilon^2}\sqrt{T^2-T_0^2} \; and \; P_4{\sim}\frac{1.8\ 10^{-5}e^2}{\lambda^2\epsilon^6}\sqrt{T^2-T_0^2} \tag{50}$$

Let us now turn to the numerical evaluation of the exponential part of the decay rate.

B. Numerical results

In order to evaluate the decay rate of the string, let us plug in the values of the linear sigma model that give rise to the observed pion mass and possible sigma mass. A simple rescaling of variables allows our effective Lagrangian to resemble the one of the linear sigma model by absorbing the electromagnetic coupling constant e^2 into a new charged field, $\tilde{\pi}_c$, and a new coupling constant $\tilde{\lambda}$. Our effective potential (6) then becomes

$$\begin{aligned} V_{eff}(\pi_c, T) &= \tfrac{e^2}{12}(T^2 - \tfrac{6\lambda\eta^2}{e^2})\pi_c^2 - \tfrac{e^3}{6\pi}T\pi_c^3 + \tfrac{\lambda}{4}\pi_c^4 \\ &= (T^2 - 6\tilde{\lambda}\eta^2)\tfrac{\tilde{\pi}_c^2}{12} - T\tfrac{\tilde{\pi}_c^3}{6\pi} + \tfrac{\tilde{\lambda}}{4}\tilde{\pi}_c^4 \end{aligned}$$

where $\tilde{\pi}_c = e\pi_c$ and $\tilde{\lambda} = \frac{\lambda}{e^4}$ are the new rescaled variables. Note that at zero temperature, this potential is exactly like the linear sigma model potential. As a result, we can use some typical values for the parameters in the linear sigma model: $\tilde{\lambda} = 10e^4$, $e^2 = \frac{4\pi}{137}$, $\eta = 66.47$ MeV. This choice of parameters corresponds to a critical temperature of $T_c = 156.2$ MeV and a minimum temperature of $T_0 = 155.936$ MeV.

TABLE I: Decay rate for $\tilde{\lambda} \sim 10$ for the spherical ($O(4)$) and cylindrical ($O(2)$) instantons for two different values of the thin-wall parameter, ϵ.

Symmetry	Action S_E	$\frac{\Gamma}{V}$ $for\ \epsilon \sim 0.1\%$	$\frac{\Gamma}{V}$ $for\ \epsilon \sim 3\%$
$O(2) \times O(2)$	$\frac{128\pi^2}{9\epsilon\lambda}$	$\sim P_2 e^{-1.7.10^6}$	$\sim P_2 e^{-5.5.10^4}$
$O(4)$	$\frac{\pi^2}{48\lambda\epsilon^3}$	$\sim P_4 e^{-2.4.10^9}$	$\sim P_4 e^{-9.0.10^4}$

As show in Table I, the exponential part of the decay rate has almost the same order of magnitude for the spherical and cylindrical case when ϵ is big enough (or equivalently, the temperature of the thermal bath of photons is closer to T_0). However, we should not forget that ϵ must be small for the thin-wall approximation to remain valid.

C. Discussion

Let us now compare the decay rates for the spherical and the cylindrical case. The ratio of the decay rate is

$$r \sim \frac{\Gamma_{sphere}}{\Gamma_{cyl}} \sim e^{-\frac{\pi^2}{\lambda\epsilon}[\frac{1}{48\lambda\epsilon^2} - \frac{128}{9}]} \tag{51}$$

Recalling that the thin wall parameter ϵ is very small, the decay rate for both configurations is very small due to the strong exponential suppression coming from the $\frac{1}{\epsilon}$ factor. Moreover, we see that the cylindrical instanton is more likely than the spherical one whenever $\epsilon < \frac{1}{32}\sqrt{\frac{3}{2}} \sim 4\%$. This is in perfect agreement with the numerical results of Table I. However, this is not what is usually expected from the symmetry argument and the spherical action, which has a bigger action, yields a smaller decay rate than the less symmetric O(2) instanton.

Let us now consider the cosmological perspective and compare the decay rate of the string per Hubble volume to the Hubble parameter. In general, if $\Gamma \sim H$ then a computation at finite temperature is necessary and for $\Gamma \ll H$ a zero temperature computation is enough. Here, the requirement for our string to be stable under breaking is that $\frac{\Gamma}{V} \ll H^4$. Roughly speaking we know that $H \sim \frac{1}{t_{QCD}}$ where $t_{QCD} \sim 10^{-5}s$ is the typical time at which the QCD phase transition occurs so that $H^4 \sim 10^{-20}s^{-4} \sim e^{-46}s^{-4}$. As obvious from Table I, the decay rate of the pion strings per unit volume is much smaller than H^4 and therefore the string is stable close to the critical temperature.

However, the thin-wall approximation is valid in a very narrow range close to the critical temperature, T_c. As one can see in Fig. 1, close to T_c, the height of the barrier, $V(\pi_c+)$, is large compared to its depth, $V(\pi_c-)$ which actually vanishes at $T = T_c$. In that case, the field value changes very quickly from inside the bubble to outside and the wall is thin: $\frac{\delta}{R} \ll 1$.

But at lower temperatures, closer to T_0, the height of the barrier of the potential becomes smaller than its depth, so that the wall becomes thicker. In that case, the height of the barrier is of order the depth of the potential and one of the minima is much lower than the other. As a result, the total potential energy contained inside the bubble is smaller and the surface term dominates since the wall is thick. We also expect a smaller action coming from the thick wall bubble yielding a smaller argument in the exponential part of the decay rate. As a consequence, for the thick wall, the prefactor includes most of the relevant information for the decay rate and we still expect a bigger decay rate than for thin-wall bubbles. So, at small enough temperature, the larger rate of bubble nucleation can make the string unstable. If it is the case, skyrmion configurations can form and expand along the string at the speed of light. This mechanism will be further developed in a follow-up paper. In this scenario, our string, which is stable at high temperature close to T_c, becomes less stable at lower temperature to end up with a classical decay below T_0.

In contrast, it is worth noting that in the sphaleron case, where only thermal fluctuation effects are considered, the colder the system is, the less likely it is to hop over the potential barrier, thus making the system more and more stable. Indeed, when all the fields are in thermal equilibrium, the decay rate goes like $\Gamma \sim e^{-\frac{S_3}{T}}$ where S_3 is the O(3) symmetric action so that a decreasing temperature exponentially suppresses bubble nucleation.

Finally, in the limit where the barrier height approaches zero, close to T_0, the bubble size approaches zero and the field classically rolls down the potential without any tunneling required so that our string vanishes.

VI. CONCLUSION

We proved that considering plasma effects on the charged fields helps stabilize the single string configuration against its decay into two strings for temperatures close to the critical temperature, T_c, and so contributes to cosmology during a certain time.

However, when the wall becomes thicker at lower temperatures, the resulting instanton action should be smaller, making the system less stable. In that case, numerical computations can be carried out in order to precisely compute the pion string decay rate without any thin-wall approximation.

Two main effects prevent the string from decaying into radially expanding configurations: Plasma pressure, and, more importantly, the string winding gradient which creates an energy barrier that encloses the core of the string. Neglecting those effects we find that the radius of the bubbles nucleated increases with temperature. However, after nucleation, we expect the bubble to be deformed and to propagate along the string at almost the speed of light. As a result, the string core melts and the two newly formed string segments move away from each other at the same speed. This melting is more likely to occur far below the critical temperature, when the string decay rate is large enough compared to the Hubble parameter.

In addition, the decay of the string has some interesting consequences: Opposite winding direction configurations for the charged fields components form skyrmion anti-skyrymion pairs when they meet. If the two configurations have the same alignment, they just pass through each other and no skyrmions form. When skyrmions form, they can spread outside the strings since cosmic strings are moving. Interpreting those skyrmions as baryons [9] [10][11], the decay of the pion string can contribute to the production of baryon-anti baryons pairs.

Finally, it is a great challenge to compute the full tunneling probability in the case where we consider the four scalar fields involved in the linear sigma model. Here we restricted ourselves to the core of the string where the neutral complex field vanishes but there are other trajectories in field space to explore in order to quantify the stability of the pion string.

Acknowledgments

We thank Robert Brandenberger for valuable discussions during this project and comments on the draft . Thanks to Ajit Mohan Srivastava for pointing out the existence of skyrmions in this model and to Mark Hertzberg for proofreading the final draft. This work was supported in part by the U.S. Department of Energy under cooperative research agreement DE-FG02-05ER-41360. The author is supported by an NSERC PDF fellowship.

---

[1] J. Karouby and R. Brandenberger, Phys. Rev. D **85**, 107702 (2012) [arXiv:1203.0073 [hep-th]].

[2] M. Nagasawa and R. H. Brandenberger, Phys. Lett. B **467**, 205 (1999) [hep-ph/9904261].

[3] G. E. Volovik, Int. Ser. Monogr. Phys. **117**, 1 (2006).

[4] S. M. H. Wong, hep-ph/0202250.

[5] A. Vilenkin and E.P.S. Shellard, *Cosmic Strings and other Topological Defects* (Cambridge Univ. Press, Cambridge, 1994).

[6] M. B. Hindmarsh and T. W. B. Kibble, "Cosmic strings," Rept. Prog. Phys. **58**, 477 (1995) [arXiv:hep-ph/9411342].

[7] R. H. Brandenberger, "Topological defects and structure formation," Int. J. Mod. Phys. A **9**, 2117 (1994) [arXiv:astro-ph/9310041].

[8] R. H. Brandenberger and X. -m. Zhang, "Anomalous global strings and primordial magnetic fields," Phys. Rev. D **59**, 081301 (1999) [hep-ph/9808306].

[9] T. H. R. Skyrme, Proc. Roy. Soc. Lond. A **260**, 127 (1961).

[10] T. H. R. Skyrme, Nucl. Phys. **31**, 556 (1962).

[11] G. S. Adkins, C. R. Nappi and E. Witten, Nucl. Phys. B **228**, 552 (1983).

[12] R. Holman, S. Hsu, T. Vachaspati and R. Watkins, Phys. Rev. D **46**, 5352 (1992) [arXiv:hep-ph/9208245].

[13] I. Dasgupta, Nucl. Phys. **B506**, 421-435 (1997). [hep-th/9702041]

[14] J. Garriga and A. Vilenkin, Phys. Rev. D **45**, 3469 (1992).

[15] J. Preskill and A. Vilenkin, Phys. Rev. D **47**, 2324 (1993) [arXiv:hep-ph/9209210].

[16] A. Monin and M. B. Voloshin, Phys. Rev. D **78**, 065048 (2008) [arXiv:0808.1693 [hep-th]].

[17] A. Monin and M. B. Voloshin, Phys. Rev. D **78**, 125029 (2008) [arXiv:0809.5286 [hep-th]].

[18] A. D. Linde, Nucl. Phys. B **216**, 421 (1983) [Erratum-ibid. B **223**, 544 (1983)].

[19] M. Quiros, arXiv:hep-ph/9901312.

[20] T. W. B. Kibble, J. Phys. A **9**, 1387 (1976).

[21] L. Dolan and R. Jackiw, Phys. Rev. D **9**, 3320 (1974).

[22] M. Dine, R. G. Leigh, P. Y. Huet, A. D. Linde, D. A. Linde, Phys. Rev. **D46**, 550-571 (1992). [hep-ph/9203203].
M. Dine, R. G. Leigh, P. Huet, A. D. Linde, D. A. Linde, Phys. Lett. **B283**, 319-325 (1992). [hep-ph/9203201].

[23] A. Achucarro and T. Vachaspati, Phys. Rept. **327**, 347 (2000) [Phys. Rept. **327**, 427 (2000)] [arXiv:hep-ph/9904229].

[24] M. Barriola, T. Vachaspati and M. Bucher, Phys. Rev. D **50**, 2819 (1994) [arXiv:hep-th/9306120].

[25] S. R. Coleman, Phys. Rev. D **15**, 2929 (1977) [Erratum-ibid. D **16**, 1248 (1977)].

[26] H. B. Nielsen and P. Olesen, Nucl. Phys. B **61**, 45 (1973).

[27] E. W. . Kolb and M. S. . Turner,

[28] C. G. . Callan and S. R. Coleman, Phys. Rev. D **16**, 1762 (1977).

[29] J. Garriga, Phys. Rev. D **49**, 5497 (1994) [arXiv:hep-th/9401020].

[30] G. V. Dunne and H. Min, Phys. Rev. D **72**, 125004 (2005) [arXiv:hep-th/0511156].